

# Effects of residual combustion gases at Elevated Pressures on Laminar Burning Velocities for Gasoline and Gasoline Surrogate

O. Mannaa<sup>1\*</sup>, M. S. Mansour<sup>1, 2\*</sup>, W. L. Roberts<sup>1</sup>, S. H. Chung<sup>1</sup>

<sup>1</sup> Clean Combustion Research Center, King Abdullah University of Science and Technology, Thuwal, Saudi Arabia

<sup>2</sup> Department of Mechanical Engineering, Helwan University, Cairo, Egypt

## Abstract

Laminar burning velocities of FACE-C (Fuels for Advanced Combustion Engines) gasoline test fuel and its developed surrogates of toluene reference fuel (TRF) (*n*-heptane, *iso*-octane, and toluene mixture) under the presence of real combustion residuals are presented. Measurements were conducted for equivalence ratios ranging from 0.8 to 1.6 using a constant volume spherical combustion vessel in the constant pressure, stable flame regime at an initial temperature of 358 K and initial pressures of 0.1 and 0.6 MPa along with tests using real combustion residuals at mole fractions of up to 0.3. For both fuels, a noticeable decrease in stretched and un-stretched flame speed was observed for flames with real combustion residuals. Furthermore, a monotonic decrease was still observed with the increase of the combustion residuals rate for slightly off stoichiometric condition ( $\phi = 1.1$ ) for both fuels. Flame stability enhancement quantified by Markstein length was achieved through the addition of real combustion residuals.

## Introduction

Despite the manifestation of recent advances in newly developing low temperature combustion engines such as HCCI and PCCI engines, gasoline combustion for propulsion, in particular for much of the world's automotive fleet still dominates. To further improve the performance of these propulsive devices, matrix of FACE gasoline fuels corresponding to different RONs have been proposed to accommodate these high efficiency advanced combustion engines (ACE) [1]. Therefore research into the combustion characteristics of these FACE gasoline fuels and its components is indispensable before commercially utilizing them. Difficult experimental and numerical characterization of these fuels typically stems from the fact that they are composed of hundreds of hydrocarbons, making them intractable to determine their burning and chemical kinetic characteristics. Therefore, it is often desirable to formulate a less complex surrogate fuels that can emulate combustion characteristics of the target multi-component fuel, which include H/C ratio, auto ignition characteristics, laminar flame speeds, engine ignition phasing, pollutant emissions, etc.[2].

One of the most important parameters of any fuels that affect significantly its burning characteristics is the laminar burning velocity. Such Physicochemical property forms an imperative parameter for turbulent combustion and ignition limits models. Moreover, it is also considered as an essential parameter for engine simulation that assesses burn duration, power output and duration of combustion [3-5]. Therefore, in order to assess the performance of these FACE fuels and their developed surrogates, it is vital to capture the associated laminar combustion characteristics, including the laminar burning velocity over a wide range of thermodynamic conditions (equivalence ratio, initial pressure and temperature) [6]. Many experimental and numerical studies have been conducted to determine the laminar flame propagation characteristics of the

individual components of gasoline surrogates [7-11]. Laminar burning velocities of *n*-heptane, *iso*-octane and toluene and various PRF mixtures have been measured at atmospheric pressure [8, 10, 11]. Bradley *et al.* [12] reported laminar burning velocities and Markstein lengths for *iso*-octane/air and *n*-heptane/*iso*-octane/air mixtures up to 1.0 MPa. Also, the flame speed of tertiary surrogates has received much attention recently [13].

Use of exhaust gas recirculation (EGR) in gasoline engines is a common method adopted mainly to reduce NO<sub>x</sub> emissions as they are quite inert and act as a non-reactive diluent in the combustion process, inducing a combustion temperature diminution and detaining the formation mechanism of NO<sub>x</sub>. It also has become one of the promising techniques to respond to the increasingly stringent standards that have mandated the reduced emission of various oxides of nitrogen (NO<sub>x</sub>). Furthermore, EGR has some potentially efficiency boosting characteristics as it induces less throttling losses, less heat losses due to wall heat transfer and reduction of endothermic dissociation reaction rates [14]. To the author's knowledge, so far with the exception of Marshall *et al.* study [15], only synthetic residuals which are mixtures of inert components have been experimentally used to simulate the effect of EGR on burning rate.

The main objective of the current study is to provide accurate data for FACE gasoline fuel (FACE-C) and its developed TRF surrogate at atmospheric and high pressure condition, but it also aims to continue breaking new ground with the studies of real combustion residuals on burning velocities. Flame stability criterion in terms of Markstein length will also be reported under the effect of combustion residuals

---

\* Corresponding authors: [Markous.Abdo@kaust.edu.sa](mailto:Markous.Abdo@kaust.edu.sa)  
[Ossama.Mannaa@kaust.edu.sa](mailto:Ossama.Mannaa@kaust.edu.sa)

## 2. Experimental Facility

A spherically stainless steel combustion vessel with 330 mm inner diameter ( $\approx 20$  liters) was employed to accommodate spherically expanding propagating flames. It is equipped with multiple optical accesses through two orthogonal pairs of quartz windows of 120 diameter and 50 mm thickness as depicted schematically in Fig.1. It is capable of withstanding the temperature and pressures generated from deflagrations at initial pressure,  $P_o$ , of up to 1.0 MPa and initial temperatures,  $T_o$ , of up to 400 K.

The vessel and mixture were heated to temperatures up to 358 K by a 1.5 kW heater located on the inner side of the bottom flange. The initial gas temperature was measured by two sheathed Chromel-Alumel thermocouples to ensure thermal homogeneity. An eight bladed fan was driven by a magnet-electric motor located at top flange to initially mix the reactants during the charging process. The presence of the fan was vital as it assures full evaporation of the liquid fuels and temperature uniformity through the vessel via the enhancement of convective heat transfer process.

The volume of liquid fuels to be injected into the vessel was calculated based on gas theory and according to the required mole composition, the liquid fuel's density, and the known inner volume of the combustion chamber. Three different sizes of calibrated gas tight micro-syringes (5, 10 and 50  $\text{cm}^3$ ) were employed during the charging process of liquid fuel inside the vessel under vacuum pressure of about 0.001 MPa, then dry air was introduced according to the initial condition ( $\phi, P_o, T_o$ ), where  $\phi$  is the equivalence ratio.

To conduct experiments with combustion residuals at wide range of equivalence ratios, a preliminary explosion corresponding to the desired equivalence ratio was performed and a portion of the combustion products were retained for the following experiment. For experiments without residuals the vessel was purged with nitrogen to scavenge combustion products remained from previous experiments.

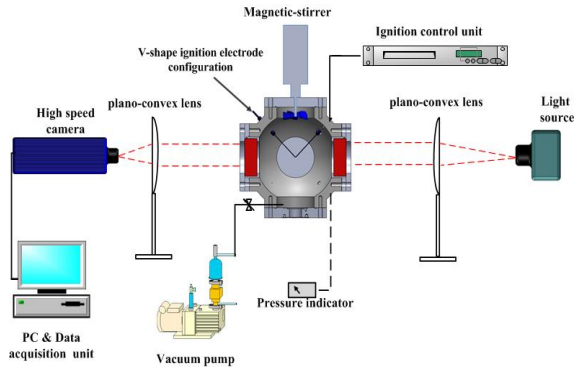


**Figure 1** Schematic of the experimental setup for the optical spherical combustion chamber.

## 3. Data analysis on spherically propagating flame

For the technique of laminar spherical flame propagations in constant volume vessel, several algebraic expressions in determining the burning velocity have been well presented in [14], involving flame radius,  $R$ , pressure,  $P$ , and time,  $t$ . Allowance must be made for the effects of the flame stretch rate,  $\kappa$ , given by  $(1/A) (dA/dt)$ , where  $A$  is the flame surface area and  $t$  is the elapsed time. For a spherical flame, this gives:

$$\kappa = (2/R_f) S_n \quad (1)$$

Where  $S_n = dR_f/dt$ , is the flame displacement speed and  $R_f$  represents the mean flame radii, obtained from a Schlieren measurement of the projected flame area. All measurements were conveniently conducted during earlier stage of near constant pressure regime. From the measured  $S_n$ , the stretched flame speed,  $S$ , free from perturbations due to ignition transient or instability by developing cellular structure was selected. The unstretched laminar flame speed,  $S_o$ , was determined from the following linear extrapolation to zero stretch:

$$S_o - S = L_b \kappa \quad (2)$$

Where  $L_b$  is the Markstein length of burnt gases, characterizing the sensitivity of flame propagation to stretch rate effects. As the combustion occurs at constant pressure for small radius, the laminar burning velocity  $u_l$  can be obtained based on the mass conservation across the flame front according the following expression:

$$u_l = S_o (\rho_b / \rho_u) \quad (3)$$

Where  $\rho_b$  and  $\rho_u$  are the burnt and unburned gas densities, respectively. Since  $dR_f/dt = u_g + S$  where  $u_g$  is the upstream gas velocity,  $\kappa$  is the sum of two contributing parameters, the aerodynamic flame strain rate effects,  $\kappa_s$ , by the upstream gas velocity and the stretch effects due to flame curvature,  $\kappa_c$ , by the flame configuration for which the expressions for both of them are given in [14].

## 4. Results and discussion

The main objective beyond this study is to investigate the effects of combustion residuals on the laminar burning velocities of FACE-C gasoline fuel and its TRF developed surrogate. Laminar flame characteristics are investigated at an initial temperature of  $T_o = 358$  and initial pressures of 0.1 and 0.6 MPa with equivalence ratio ranging from 0.8 to 1.6 along with tests using real combustion residuals at mole fraction of 0.1. Then, impact of the variation of combustions residuals mole fraction will be examined for slightly off-stoichiometric condition ( $\phi = 1.1$ ) for both fuels Furthermore, the effect of combustion

residuals on flame stability will be assessed through Markstein length.

#### 4.1 Validation of combustion chamber

To assess the validity of the experimental facility and methodology employed in this study, some obtained results of unstretched laminar burning velocity,  $u_l$ , were compared with data from literature [7, 11, 16-18] for pure *n*-heptane/air flame at  $P_0 = 0.1$  MPa and  $T_0 = 300$  K as depicted in Fig.2. The displayed results of  $u_l$  for *n*-heptane/air flames show a satisfactory agreement between the current work's measurements and others, although some of them were obtained from different flame configurations.

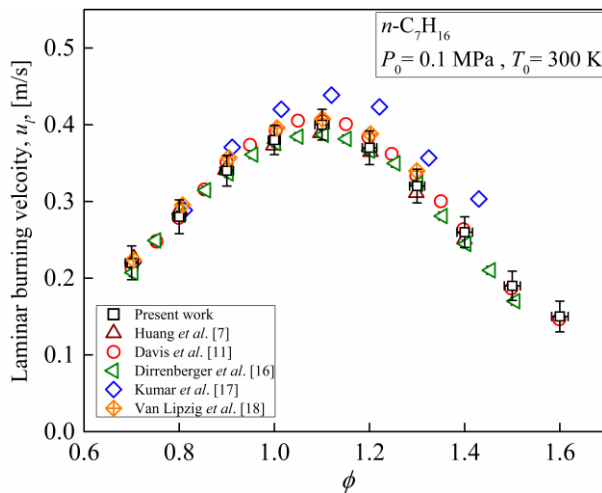


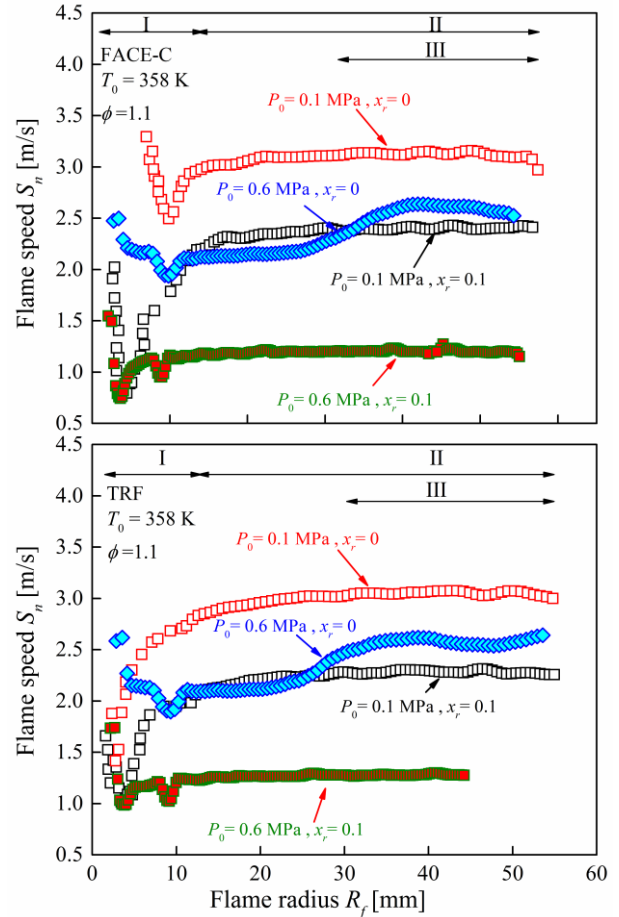
**Figure 2** Present values of  $u_l$  for *n*-heptane flames at  $P_0 = 0.1$  MPa and  $T_0 = 300$  K, compared with previous studies in the literature.

#### 4.2 Flame speeds of FACE-C gasoline and its surrogate with and without residuals.

Typical variations of flame speed,  $S_n$ , with temporal evolution of flame radii are shown in Fig.3 for FACE-C (a) gasoline and its TRF developed surrogate (b) at  $T_0 = 358$  K and  $P_0 = 0.1$  and  $0.6$  MPa for  $\phi = 1.0$ . These exhibit the response of stretched flame speeds with respect to flame radii for FACE-C and its TRF developed surrogate, respectively. As depicted in Fig.3, regime I shows over-driven flame speeds that resulted from the deposition of excessive energy from the spark-ignited flame kernel, a well-known experimental phenomenon [19]. Afterwards, after the recovery of the flame from attaining a minimum value as shown in Fig.3, the normal flame chemistry develops recovering from the ignition transient regime. Such normal flame chemistry is characterized by the linear response of stretched flame speeds with respect to stretch rate which controls the bounds of linear extrapolation of stretched flame speed to a zero stretch rate to obtain  $S_0$ . For high pressure and heavy rich hydrocarbon flames,  $S_n$  has the propensity to increase significantly at later stages of

propagation due to flame instability triggered by the full development of a cellular flame surface.

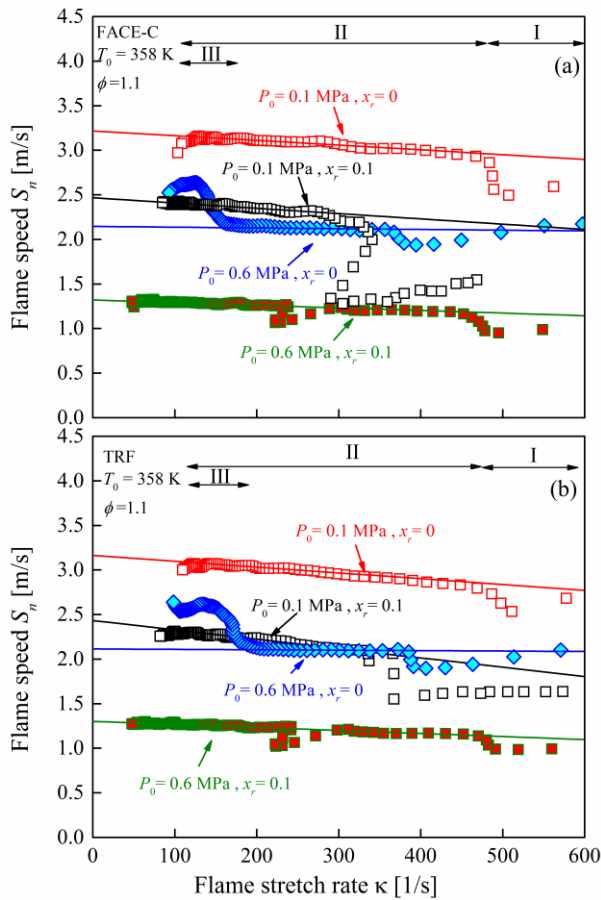
Thus, spherical flame propagation can be kinematically distinctive throughout three different regimes; regime I for ignition transient, regime II for stable normal flame chemistry propagation and regime III for unstable accelerated cellular flame. These aforementioned regimes can be clearly manifested through the dependence of flame speed on stretch rate as shown in Fig.4. In regime I, the enhanced flame



**Figure 3** Variations of flame speeds,  $S_n$ , with  $R_f$  for (a) FACE-C and (b) its developed TRF surrogate at  $T_0 = 358$  K and  $P_0 = 0.1$  &  $0.6$  MPa for  $\phi = 1.1$ .

speed due to ignition energy effect deteriorates for flame radii larger than 6 to 10 mm [20]. In regime II, the flame propagation starts its linear response to stretch rate which will be used to obtain both the Markstein length,  $L_b$ , and the unstretched laminar burning velocity,  $u_l$ . In regime III the flame speed encounters a sudden acceleration as shown in Fig. 4b due to full development of cellularity that causes an increase in the flame surface area, and in turns the burning rate also increases. Figs 4 and 5 clearly depict the interaction examined between the effects of combustion residuals composition on the laminar burning velocities of real FACE-C gasoline /air mixture and its TRF developed surrogate. A mole fraction of  $x_r = 0.1$  causes about 33 %

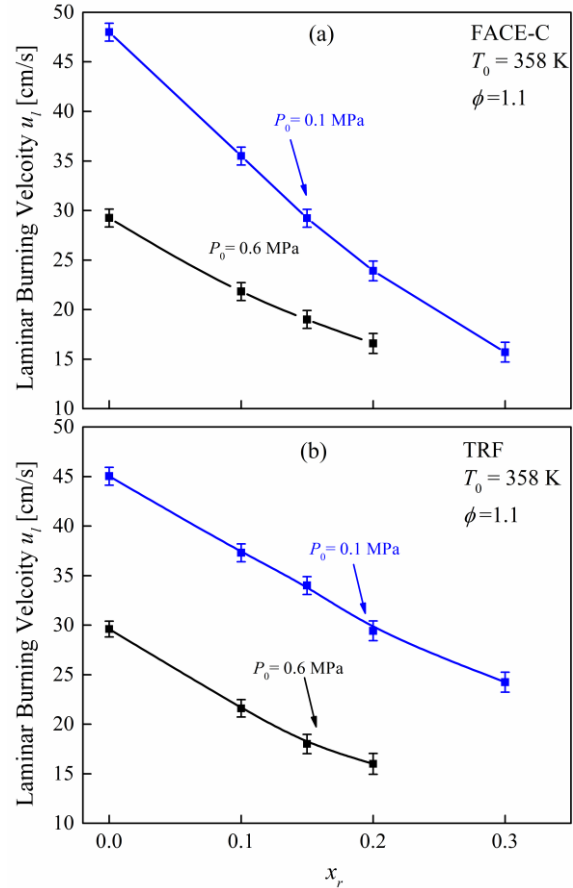
and 50 % decrease of slightly off stoichiometric flame speed ( $\phi = 1.1$ ) at 0.1 and 0.6 MPa, respectively compared with the flame speed without combustion residuals. Such anticipated trend can be simply attributed to the overall reduction in  $O_2$  concentration in the combustion gases and the composition of the diluent and non-diluent gases in the combustion residuals. Furthermore, the presence of high specific heat capacity diluent species such as  $N_2$  or tri-atomic molecules as  $CO_2$  or  $H_2O$  lowers the heat release of the mixture per unit volume and the probability of fuel molecule to be attacked by oxidizer molecule. Therefore the local peak temperature in the flame is decreased within the reaction zone, which in turn will induce significant reduction in the laminar burning velocity. Noticeably, the examined interaction between flames with and without exhaust residuals can be clearly manifested through regime III. As previously mentioned, regime III characterizes the unstable flame morphology in terms of formation of cellular structure that causes sudden acceleration of flame speeds, and as clearly shown in Figs, 4 and 5 the presence of exhaust gases during combustion hinder the inception of such regime. In other words, flame stability is enhanced by the addition of exhaust gases during the combustion process.



**Figure 4** Variations of flame speeds,  $S_n$ , with flame stretch rate,  $\kappa$ , for (a) FACE-C and (b) its developed TRF surrogate at  $T_0 = 358$  K and  $P_0 = 0.1$  & 0.6 MPa for  $\phi = 1.1$ .

### 4.3 Effect of different EGR mole fractions on laminar burning velocity

The interaction between the effect of variable mole fractions of combustion residuals and laminar burning velocities of FACE-C and its developed TRF surrogate is examined below.



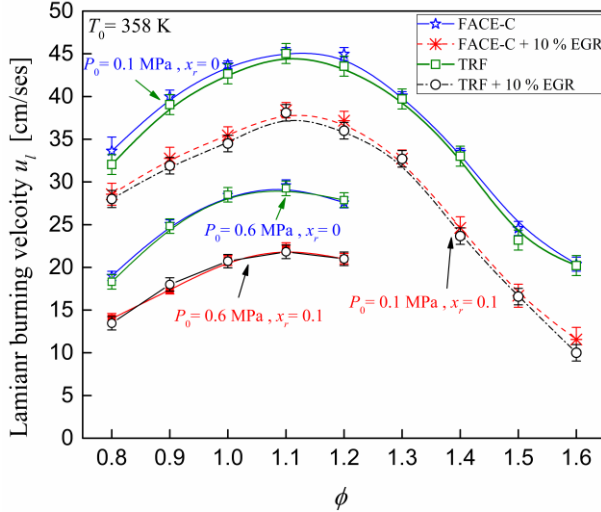
**Figure 5** Variations of laminar burning velocity,  $u_l$ , with increasing EGR mole fraction for (a) FACE-C and (b) its developed TRF surrogate at  $T_0 = 358$  K and  $P_0 = 0.1$  & 0.6 MPa for  $\phi = 1.1$ .

Fig.5 depicts the variation of laminar burning velocity of FACE-C and its surrogate with different mole fractions of combustion residuals. The monotonic reduction of burning velocity with increasing the mole fraction of EGR is expected. As explained above, this can be attributed to the decrease in the flame temperature as more combustion residuals are added. Increasing the EGR mole fraction results in a significant increase in the specific heat capacity of the mixture compared with conventional combustion, which in turn lowers the burning rate of the mixture. Furthermore, for atmospheric measurements, the reduction in flame speed caused by different exhaust residuals portions is, to some extent, more pronounced compared with their counterparts at high pressure condition. This suggest that that addition of EGR may not strictly cause thermodynamic alteration in the system, but also can cause chemical kinetic effect as predicted by [21]. In Fuller *et.al* study [21], it was suggested that the presence of  $CO_2$  which is abundant species in

combustion residuals may adversely affect the overall radical concentration resulting from chain-branching reactions.

#### 4.4. Laminar burning velocities

Fig.6 exhibits the unstretched laminar burning velocities versus a wide range of equivalence ratios with and without exhaust residuals for FACE-C and its surrogate. Seemingly, the reduction in unstretched laminar burning velocity caused by 10 % EGR is, to some extent has a weak dependence on the equivalence ratio for both fuels regardless of the initial pressure condition.



**Figure 6** Variations of unstretched laminar burning velocities,  $u_l$ , with  $\phi$  for FACE-C and its developed TRF surrogate with and without EGR at  $T_0 = 358$  K and  $P_0 = 0.1$  &  $0.6$  MPa.

#### 4.5. Interaction of combustion residuals with flame instability assessment

Flame instability was assessed through the estimation of Markstein length extracted from the slope of linear regime II (refer to Fig.4) using Eq.2. Fig.7 shows the variation of Markstein length for FACE-C and its surrogate at initial pressures of 0.1 and 0.6 MPa with equivalence ratios for flames with and without residuals. Since the target fuels belong to heavy hydrocarbons, the Markstein length of both fuels with and without residuals will decrease monotonously with the increase of equivalence ratio. Moreover, as depicted in Fig.7, Markstein lengths for mixtures with exhaust residuals increase significantly compared with their counterparts without combustion residuals. This reveals that EGR flames maintain higher stability compared to non-EGR flames and the addition of EGR can increase the flame front stability. The smaller the Markstein length is indicative of the less important the influence of stretch on laminar burning velocity. As a consequence, combustion residuals promote the effect of stretch on flame propagation. Noticeably, the increment of Markstein length with 10 % of EGR is larger in the lean mixtures than that in the rich ones. Hence, it can be

deduced that the addition of EGR has more pronounced influence on flame stability for lean flames.

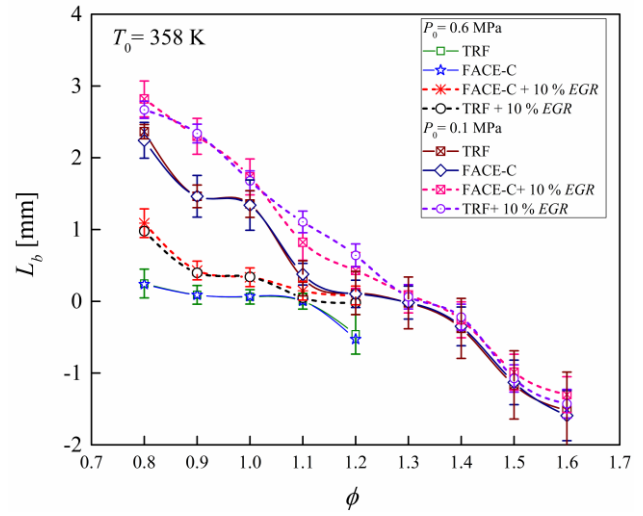


**Figure 7** Variation of present values of  $L_b$  with  $\phi$  for FACE-C gasoline fuel and its TRF developed surrogate mixtures with and without exhaust residuals at 358 K initial pressures of 0.1, and 0.6 MPa.

#### 5. Conclusion

Measurements of laminar burning velocities of FACE-C gasoline fuel and its developed TRF surrogate have been conducted at initial temperature of 358 K and initial pressures of 0.1 and 0.6 MPa. The measurements include tests using real combustion residuals to investigate the effect of EGR on combustion process and provide data that can be used for validation in the realm of vitiated kinetics. The present results exhibit a weak dependence of the reduction associated with the laminar burning velocities of FACE-C gasoline and its TRF surrogate flames with real combustion residuals on the mixture's stoichiometry. Such reduction was justified based on the increase of heat capacity of combustion residuals and tri-atomic molecules dissociation such as carbon dioxide. By considering the burning rate (i.e.,  $\rho_u \cdot u_l$ , with  $\rho_u$  the fresh gas density) a continuous decrease in the laminar burning velocities is still observed with the increase of dilution caused by the presence of real combustion residuals. With respect to flame stability, for both fuels the combustion residuals promote flame stability indicated by a noticeable increase in the Markstein length, in particular for lean flames.

#### Acknowledgement

This work was supported by the FUELCOM program funded by Saudi Aramco.

#### References

- [1] S. M. Sarathy; G. Kukkadapu; M. Mehl; W. Wang; T. Javed; S. Park; M. A. Oehlschlaeger; A. Farooq; W. J. Pitz; C.-J. Sung, Proceedings of the Combustion Institute (2014).

- [2] W. J. Pitz; N. P. Cernansky; F. L. Dryer; F. Egolfopoulos; J. Farrell; D. Friend; H. Pitsch, in: SAE Technical Paper: 2007.
- [3] J. T. Farrell; W. Weissman; R. J. Johnston; J. Nishimura; T. Ueda; Y. Iwashita, in: SAE Technical Paper: 2003.
- [4] F. Bonatesta; P. Shayler, Proceedings of the Institution of Mechanical Engineers, Part D: Journal of Automobile Engineering 222 (11) (2008) 2147-2158
- [5] F. Lindström; H.-E. Angstrom; G. Kalghatgi; C. E. Möller, in: SAE Technical Paper: 2005.
- [6] T. M. Foong; K. J. Morganti; M. J. Brear; G. da Silva; Y. Yang; F. L. Dryer, Fuel 115 (2014) 727-739.
- [7] Y. Huang; C.-J. Sung; J. Eng in: *Determination of laminar flame speeds of primary reference fuel and reformer gas mixtures using digital particle image velocimetry*, 42nd AIAA Aerospace Sciences Meeting and Exhibit, 2004; 2004; pp 3398-3408.
- [8] L. Sileghem; V. Alekseev; J. Vancoillie; E. Nilsson; S. Verhelst; A. Konnov, Fuel 115 (2014) 32-40.
- [9] D. Bradley; M. Lawes; K. Liu; S. Verhelst; R. Woolley, Combustion and Flame 149 (1) (2007) 162-172.
- [10] T. Dubois; N. Chaumeix; C.-E. Paillard, Energy & Fuels 23 (5) (2009) 2453-2466.
- [11] S. Davis; C. Law, Combustion Science and Technology 140 (1-6) (1998) 427-449.
- [12] D. Bradley; M. Lawes; M. Mansour, Combustion and Flame 156 (7) (2009) 1462-1470.
- [13] S. Jerzembeck; N. Peters; P. Pepiot-Desjardins; H. Pitsch, Combustion and Flame 156 (2) (2009) 292-301.
- [14] P. Dimopoulos; C. Rechsteiner; P. Soltic; C. Laemmle; K. Boulouchos, International journal of hydrogen energy 32 (14) (2007) 3073-3083.
- [15] S. Marshall; S. Taylor; C. Stone; T. Davies; R. Cracknell, Combustion and Flame 158 (10) (2011) 1920-1932.
- [16] P. Dirrenberger; P.-A. Glaude; R. Bounaceur; H. Le Gall; A. P. da Cruz; A. Konnov; F. Battin-Leclerc, Fuel 115 (2014) 162-169.
- [17] K. Kumar; J. Freeh; C. Sung; Y. Huang, Journal of propulsion and power 23 (2) (2007) 428-436.
- [18] J. Van Lipzig; E. Nilsson; L. De Goey; A. Konnov, Fuel 90 (8) (2011) 2773-2781.
- [19] D. Bradley; C. Sheppard; I. Suardjaja; R. Woolley, Combustion and Flame 138 (1) (2004) 55-77.
- [20] D. Bradley; P. Gaskell; X. Gu, Combustion and Flame 104 (1) (1996) 176-198.
- [21] C. Fuller; P. Gokulakrishnan; M. Klassen; S. Adusumilli; Y. Kochar; D. Bloomer; J. Seitzman; H. H. Kim; S. H. Won; F. Dryer in: *Effects of vitiation and pressure on laminar flame speeds of n-decane*, AIAA 50th Aerospace Science Meeting, 2012; 2012.